


3-Dimensional Biomechanics of Noncontact Anterior Cruciate Ligament Injuries in Male Professional Soccer Players

Matteo Zago,^{*†} PhD , Fabio Esposito,[†] MD, Susanna Stillavato,[†] BME, Stefano Zaffagnini,[‡] MD, Carlo Albino Frigo,[§] PhD, and Francesco Della Villa,^{||} MD
Investigation performed at the Education and Research Department, Isokinetic Medical Group, FIFA Medical Centre of Excellence, Bologna, Italy, and Sport and Exercise Science Faculty, Department of Biomedical Sciences for Health, Università degli Studi di Milano, Milano, Italy

Background: The understanding of noncontact anterior cruciate ligament (ACL) injury causation in soccer has improved over the past decades. Bidimensional video analyses have significantly augmented our awareness, representing to date the only practical method to describe injury biomechanics. However, the extent of the problem continues to raise serious concerns.

Purpose: To advance our understanding of the causal pathways leading to ACL injury with a large-scale reconstruction of 3-dimensional (3D) whole-body joint kinematics of injuries that occurred to male elite soccer players, as well as to compare the joint angle time course among situational patterns.

Study Design: Descriptive laboratory study.

Methods: A total of 33 consecutive noncontact and indirect contact ACL injuries that occurred in 6 national and 2 international professional leagues (seasons 2020-2021 to 2022-2023 until December 2022) were analyzed: (1) multiview noncoaxial television images were inspected; (2) multiple camera views were taken from 400 ms before the initial ground contact to 200 ms after the injury frame; (3) a size-matched pitch was modeled and used to calibrate cameras; (4) a 3D skeletal model was adjusted to fit the player's pose in each frame/view; and (5) poses were interpolated, and Euler joint angles were extracted.

Results: The authors reconstructed the 3D lower limb joint kinematic curves preceding and during ACL injuries in 33 cases; notably, a sudden external (up to 5°) and then internal knee rotation was observed after the initial contact and before the injury frame. The overall kinematics at injury were knee moderately flexed ($45.9^\circ \pm 21.7^\circ$), abducted ($4.3^\circ \pm 5.1^\circ$), and externally rotated ($3.0^\circ \pm 6.4^\circ$); trunk shallowly flexed ($17.4^\circ \pm 12.5^\circ$) and rotated and tilted toward the injured side; and hip flexed ($32.0^\circ \pm 18.7^\circ$), abducted ($31.1^\circ \pm 12.0^\circ$), and slightly internally rotated ($6.6^\circ \pm 12.2^\circ$). Variable behaviors were observed at the ankle level.

Conclusion: Via reconstruction of the sequence of whole-body joint motion leading to injury, we confirmed the accepted gross biomechanics (dynamic valgus trend). This study significantly enriches the current knowledge on multiplanar kinematic features (transverse and coronal plane rotations). Furthermore, it was shown that ACL injuries in male professional soccer players manifest through distinct biomechanical footprints related to the concurrent game situation.

Clinical Relevance: Interventions aimed at reducing ACL injuries in soccer should consider that environmental features (ie, situational patterns) affect injury mechanics.

Keywords: ACL; biomechanics; soccer medicine; injury prevention; kinematics

The understanding of anterior cruciate ligament (ACL) injury causation in soccer has significantly improved over the past decades: noncontact and indirect contact injury mechanisms have received the most attention, as they are considered preventable. Single-leg landing and unanticipated sidestepping best represent the noncontact injury scenario. Biomechanically, a combination of externally applied knee flexion, valgus, and internal rotation moments elevate

ACL strain and are related to injury risk.^{14,32,37} Discipline- and sex-specific patterns have been identified, and the gross biomechanics have been extracted by video analysis studies.^{8,15,23,24,27} Noncontact ACL injuries are now considered sensorimotor failures,^{2,11} as the body's kinematics during injury results from morphological, physiological, cognitive, and emotional factors striving to keep body structures within the boundaries of admissible variability in a complex dynamic environment.^{1,3,29}

When the community adopts prevention programs, the process loops back to epidemiological campaigns: from 2001-2002 to 2018-2019 there was a seasonal 4% decrease in incidence of ligament injuries in elite European soccer.¹⁰

Still, the extent of the problem raises serious concerns: ligament injury severity (from 181 to 242 days of absence) increased by 2% to 4% over the same period, with the second highest estimated economic burden for the clubs at €85,000 per 1000 hours of exposure.³⁰

The primary aim of this study was to advance our understanding of the pathomechanics of ACL injuries in male professional soccer players. A secondary aim was to compare the time course of joint kinematics of injurious actions among different situational patterns (ie, different types of concurrent game situations) to clarify the extent to which the environment affects body postural arrangements before and during an ACL injury. We leverage an approach that stands between classic video analysis and *in silico* modeling: the model-based image matching (MBIM) technique.^{18,19,21} This method enables a realistic reconstruction of 3-dimensional (3D) whole-body joint kinematics of injuries in real-world conditions.

METHODS

Study Design

This cross-sectional observational study involved a systematic search of online database resources spanning 3 seasons (2020-2021, 2021-2022, and 2022-2023 until December 2022). The search aimed to identify ACL injuries occurring during national (English Premier League, Spanish La Liga, French Ligue 1, German Bundesliga, Italian Serie A, USA Major League Soccer) and international (UEFA Nations League, FIFA World Cup Qatar 2022) competitions.

To identify ACL injuries, we extracted team rosters and then searched each player's performance and injury history on web database resources.³⁵ We extended this data-seeking approach to additional online repositories to capture any potential injuries that might have been overlooked. Injuries were only included when we could confirm them via an official press release by the clubs' medical staff stating the nature of the injury as a complete ACL rupture. At this stage, 47 injuries were retained.

Video Collection and Data Extraction

Video recordings of the matches were obtained from an extensive online repository (Wyscout). Once retrieved, the injury clip was evaluated to ensure it was suitable for subsequent multilevel analysis (Appendix Figure A1, depicts the inclusion flowchart, available in the online version of this article). The selected recordings were downloaded

and then processed using Kinovea (Version 0.8.15; Kinovea open-source project), which allowed for accurate frame-by-frame navigation. The videos were recorded at a standard television frame rate, that is, 25 to 30 frames per second. As secondary (or third) views, we used slowed-down replays, and the equivalent effective frame rate was increased accordingly, which typically had frame rates ranging from 100 to 240 frames per second, depending on the source and broadcasting specifications. Each video was trimmed from approximately 5 seconds before to 3 seconds after the suspected injury frame (IF). IF was estimated after initial contact (IC) from the collegial observation of pathognomonic signs such as (1) a sudden, aberrant relative femorotibial displacement attributable to the compromised ligamentous support and (2) concomitant with the ligamentous rupture, a notable cocontraction of the surrounding musculature, including the quadriceps and hamstrings, in an attempt to stabilize the compromised joint. The process included reaching a consensus on the identified IF by 2 trained observers (S.S., M.Z.).

Ethics Considerations

All video material accessed is publicly available, and data were treated with confidentiality. Because no personal player information was accessed, ethics approval was not required.

Identification of Injury Mechanism, Situational Pattern, and Environmental Information

We adopted the same research framework of recently published video analyses,^{8,24} with the first layer being the injury mechanism (direct contact, indirect contact, or noncontact), the second layer representing the situational pattern, and the third layer focusing on injury biomechanics. The playing phase, either defensive or offensive, was defined and categorized based on ball possession. All available television views were then used to determine the injury mechanism and soccer-specific situational pattern, as described in a previous paper by our group.⁸ Qualitative injury description also included the player's position on the pitch and other environmental variables, such as date of injury, time during the game when the injury occurred, minutes played by the injured athlete, and injury location on the pitch.⁸

Biomechanical Analysis

Kinematic analysis was performed at IC and IF for both indirect and noncontact injuries, when permitted by the

*Address correspondence to Matteo Zago, PhD, Department of Biomedical Sciences for Health, Università degli Studi di Milano, Via Colombo 71, Milano, 20133, Italy (email: matteo.zago@unimi.it).

[†]Department of Biomedical Sciences for Health, Università degli Studi di Milano, Milano, Italy.

[‡]Clinica Ortopedica e Traumatologica II, IRCCS Istituto Ortopedico Rizzoli, Bologna, Italy.

[§]Dipartimento di Elettronica, Informazione e Bioingegneria, Politecnico di Milano, Milano, Italy.

^{||}Education and Research Department, Isokinetic Medical Group, FIFA Medical Centre of Excellence, Bologna, Italy.

Submitted September 11, 2023; accepted March 7, 2024.

The authors declared that they have no conflicts of interest in the authorship and publication of this contribution. AOSM checks author disclosures against the Open Payments Database (OPD). AOSM has not conducted an independent investigation on the OPD and disclaims any liability or responsibility relating thereto.



Figure 1. Model matching of an injury that occurred in a pressing situation (the most represented class). Relevant frames are displayed. IC, initial contact; IC-1, the modelled frame preceding the initial contact; IF, injury frame; IF+1, the modelled frame subsequent to the injury frame.

image quality. For the biomechanical analysis to be conducted, videos had to meet certain criteria; namely, ≥ 2 perspective (noncoaxial) views of the injured athlete, approximately the sagittal (lateral) and frontal (anterior or posterior) views and an unobscured view of the athlete and of the foot contacting the ground,⁴ and the existence of enough frames for the analysis of the predefined time window on all views. IF was visually determined considering pathognomonic cues.

A photogrammetric technique known as MBIM was employed to reconstruct the 3D joint kinematics during the action.^{9,20,21} The 3D modeling software used was Blender (Version 2.90; Blender Foundation) and its add-on fSpy (Version 1.0.3) for camera calibration.

Initially, a 3D model of the soccer pitch reproducing its real-world dimensions (usually 105×68 m) was constructed and used as a reference object. The global reference system was positioned at midfield, with the x (y) axis parallel to the long (short) side of the pitch and the z axis pointing upward.

Second, 9 unevenly separated key frames were selected that corresponded to clearly identifiable key events, such as an injured player's foot strike or penultimate step toe-off, ball bouncing, or other distinct actions.⁹ These events made it possible to synchronize the different video recordings. Then, the camera calibration parameters (position, orientation, focal length) were estimated with fSpy based on the convergence of the parallel lines and then imported

into Blender. Minor manual adjustments of the camera settings were required to match the reference object.

Third, a rigged full-body skeleton model containing 39 rigid segments joined to each other by 30 rotational joints, with a hierarchical structure, was scaled based on the athlete's height and weight in the calibrated 3D space. At each key frame, the model was matched with the camera views, starting with the pelvis as the parent segment and then proceeding from proximal to distal segments (Figure 1). A total of 3 translational and 93 rotational degrees of freedom (3×30 joints + 3 defining the pelvis orientation) were adjusted: 24 for the upper body; 27 for the pelvis and lower body; and 42 for the trunk, neck, and head.

Last, cubic Bézier curves were used to interpolate the kinematic parameters of the poses to obtain a continuum between the key frames. A custom Python script was used to extract angular kinematics (expressed as ZYX Euler rotations according to the International Society of Biomechanics recommendations³⁹) of the pelvis and injured lower limb; trunk kinematics was obtained by combining the relative orientation of the 3 segments modeling the spine (T1-T8, T9-L2, and L3-sacrum). Animations and related plots were generated from 400 ms before to 200 ms after IF. The trajectory of the body center of mass was also provided via the modeling software (Blender). The adopted approach closely matches the procedures explained by Koga and colleagues,^{18,19} from key frame selection and synchronization, to camera calibration, to posture matching. To further

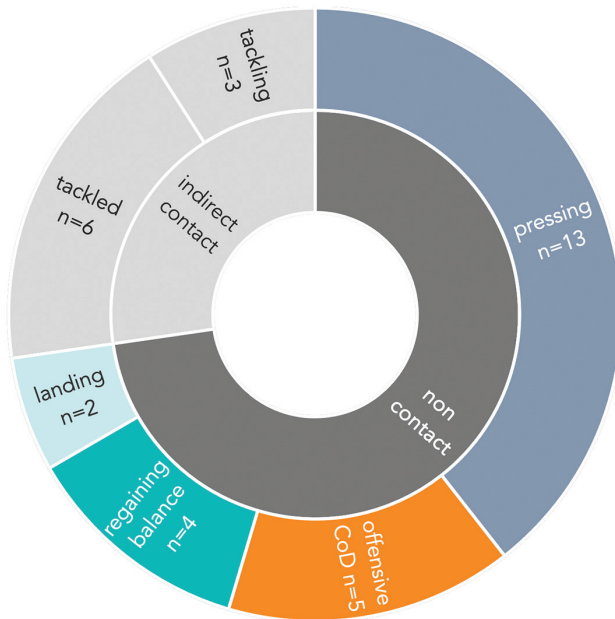


Figure 2. Multilayer classification of the included cases. Inner ring, injury mechanics; outer ring, situational pattern. CoD, change of direction.

advance the method, we adopted an automated tool (fSpy) to assist in camera parameter definition and for use with the contemporary modeling software.

Statistical Analysis

Descriptive statistics are presented as frequencies (absolute and percentage). Chi-square tests were used to compare categorical distributions within relevant domains.

Differences in dependent variables (ie, kinematic waveforms) between situational patterns were tested using Statistical Parametric Mapping (www.spm1d.org) 1-dimensional analysis of variance, with Bonferroni-adjusted post hoc comparisons where appropriate.^{28,40} Rather than limiting the analysis to arbitrarily selected discrete time points, this approach allowed the identification of statistically significant differences across the entire duration of the time series, providing solid quantitative details about the timing of observed differences among families of curves.

An a priori statistically significant level of $P < .05$ was used. Analyses were performed within MATLAB (Version 2020b; MathWorks Inc).

RESULTS

Initially, 47 ACL injuries were included in the analysis. Video footage was available and suitable for situational pattern and injury mechanism analysis in 33 cases (Appendix Figure A1, available online).

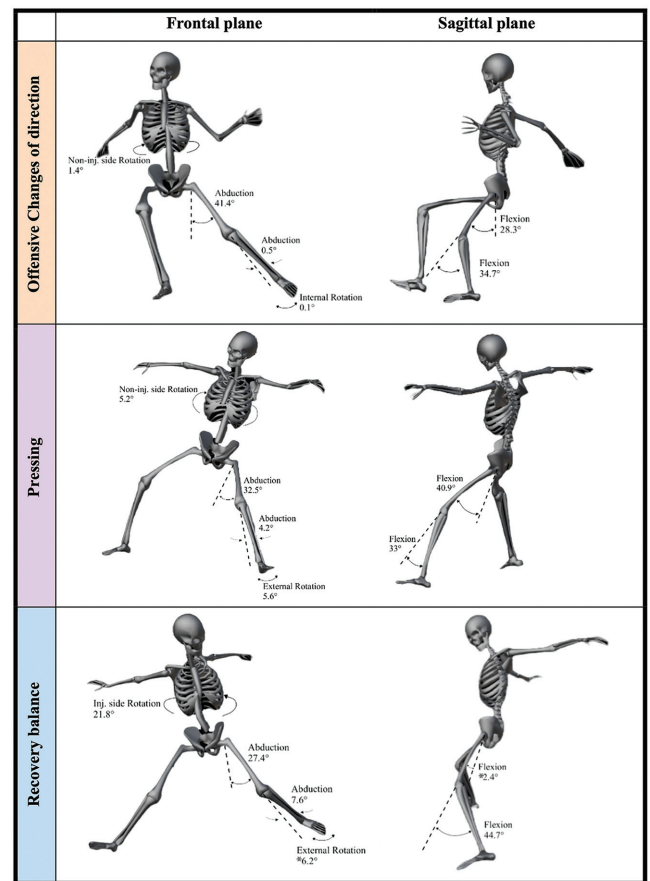


Figure 3. Representative postures at the initial contact in the 3 considered situational patterns (left injured [Inj] limb). Frontal (left) and sagittal (right) plane views are provided. *Concurrent significant differences between patterns in the time series (see Figures 4-7).

Injury Mechanism

Of the 33 cases included, 24 (73%) were noncontact and 9 (27%) were indirect contact injuries (Figure 2). Indirect contact injuries happened mostly after a mechanical perturbation on the upper body (7 of 9; $P = .002$).

Situational Pattern

Injuries occurred evenly in offensive (48%) and defensive (52%) situations ($P > .99$). Indirect contact injuries always involved a dual-type interaction, such as tackling or being tackled. Noncontact injuries primarily occurred during pressing actions (54%), followed by offensive changes of direction (CoDs) (21%), regaining balance after kicking (17%), and landing from jumps (8%).

Three-Dimensional Biomechanical Analysis of Noncontact ACL Injuries

In our sample, the vast majority of injuries occurred with a single foot in contact with the ground at 1F ($n = 26$;

TABLE 1
Discrete Joint Kinematics at IC and at Suspected IF^a

Joint/Segment	Movement	IC, deg	IF, deg	Interpretation
Trunk	Flexion	15.1 (11.9)	17.4 (12.5)	Shallow forward trunk flexion
	Axial rotation	4.6 (20.8)	7.4 (21.0)	Rotation trend toward the injured side
	Lateral bend	5.4 (12.5)	7.9 (13.2)	Trunk tilted on the injured side
Hip	Flexion	35.0 (19.4)	32.0 (18.7)	Moderately flexed hip
	Adduction	30.6 (13.4)	31.1 (12.0)	Abducted hip
	Rotation	-1.2 (10.7)	-6.6 (12.2)	Slightly internally rotated hip
Knee	Flexion	41.9 (21.5)	45.9 (21.7)	Knee slightly to moderately flexed
	Abduction	2.0 (5.0)	4.3 (5.1)	Global abducted (valgus) knee trend
	Rotation	1.6 (5.3)	3.0 (6.4)	Mostly externally rotated knee
Ankle	Plantarflexion	5.2 (14.1)	4.3 (13.6)	Mostly plantarflexed, with variability
	Supination	-0.4 (7.9)	0.5 (8.1)	Sparse behavior
	Rotation	0.6 (8.9)	0.6 (8.6)	Globally neutral/external rotation trend

^aValues are presented as mean (SD). IC, initial contact; IF, injury frame.

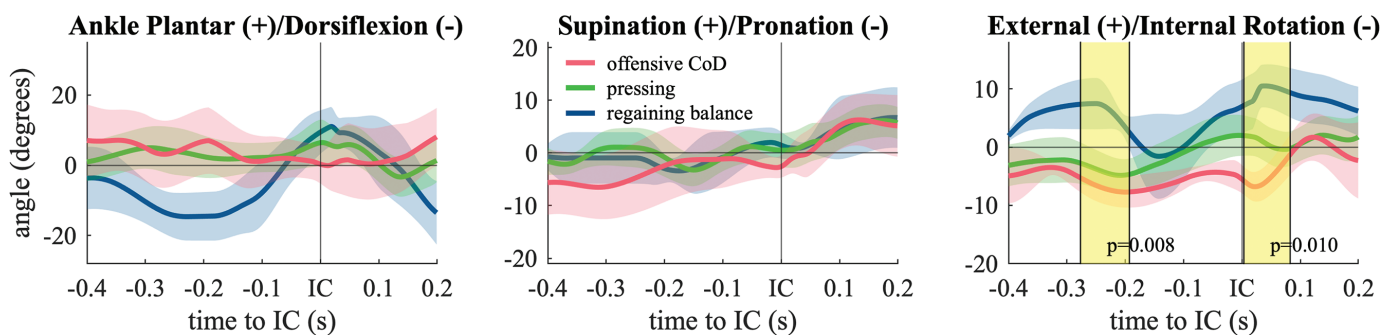


Figure 4. Ankle joint kinematics (mean and SD) in the (left) sagittal, (center) frontal, and (right) transverse planes. Colors refer to separate situational patterns. Shaded bars indicate significant differences between patterns (1-dimensional analysis of variance). CoD, change of direction; IC, initial contact.

79%; $P < .001$). ACL ruptures were fairly evenly split between the kicking (preferred) leg (52%) and the nonkicking (nonpreferred) leg (48%), with a dynamic knee valgus (combination of knee external rotation, abduction, and potentially flexion and hip adduction) observed in 22 of the 33 cases (67%). At IC, the foot strike was predominantly with the heel ($n = 19$; 58%; $P < .001$) or, less commonly, with the midfoot ($n = 4$; 12%). Further details are reported in the Appendix Table 3 (available online). All pressing and offensive CoD injuries happened during side-stepping movements, while all the recovery balance injuries were defined as planting maneuvers⁸ (foot in full contact with the ground during braking or abrupt CoD).

Figure 3 shows representative total-body postures at IC, and Table 1 presents an overview of the joint kinematics from IC to IF (mean, 42 ± 26 ms). Subsequent kinematic descriptions proceed up the kinetic chain, moving from the ankle of the injured limb to the trunk, as depicted in Figures 4 to 7.

Ankle Joint. In regaining balance injuries, we observed a shift from ankle dorsiflexion (possibly during an aerial prelanding phase) followed by ankle plantarflexion after ground contact (Figure 4). At IC, the ankle exhibited slight plantarflexion ($6.4^\circ \pm 4.9^\circ$) during pressing injuries and

increased mean plantarflexion ($9.3^\circ \pm 6.2^\circ$) in regaining balance injuries, while being substantially neutral (neither plantarflexed nor dorsiflexed) during offensive CoDs.

In the frontal plane, no significant differences were found between situational patterns; we observed a general shift toward ankle supination after IC.

While regaining balance, the ankle was found to be significantly more externally rotated (about 8° - 10°) compared with the other 2 patterns. This difference was observed from both 276 and 192 ms before IC ($P = .008$) and from IC to 83 ms afterward ($P = .010$). There, in offensive CoDs, the ankle was internally rotated ($-6.0^\circ \pm 2.3^\circ$).

Knee Joint. The time course of knee kinematics remained consistent across the 3 patterns (Figure 5), without significant differences before 0.1 second after IC. At IC, knee flexion was 37.2° to 45.2° (mean, $41.9^\circ \pm 21.5^\circ$); knee flexion increased after 40 ms after IC in pressing and regaining balance injuries, while in offensive CoDs, it remained almost stable up to approximately 150 ms after IC (approximately 40° vs 60° ; $P = .037$).

Starting from -50 ms and continuing to 100 ms after IC, the knee was progressively abducted (moving from a neutral or slightly varus angle to about $8.0^\circ \pm 4.1^\circ$ of knee valgus) before returning to a neutral alignment

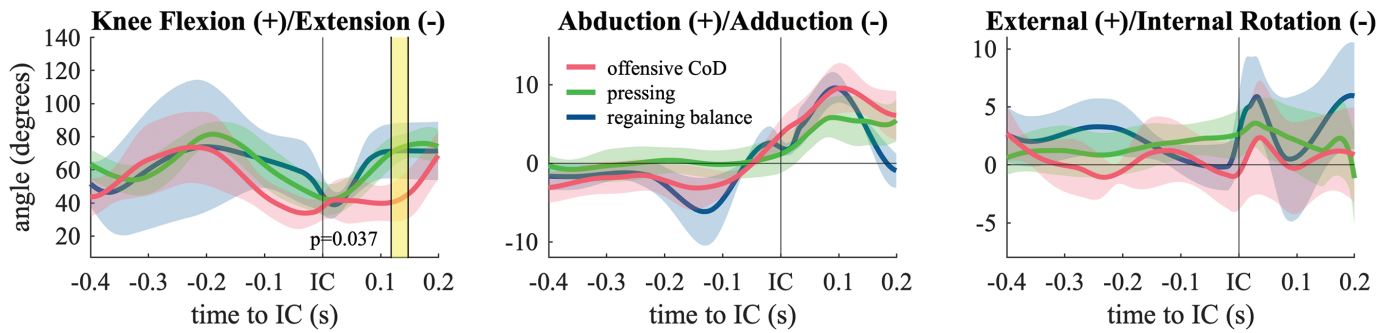


Figure 5. Knee joint kinematics (mean and SD) in the (left) sagittal, (center) frontal, and (right) transverse planes. Colors refer to separate situational patterns. Shaded bar indicates significant differences between patterns (1-dimensional analysis of variance). CoD, change of direction; IC, initial contact.

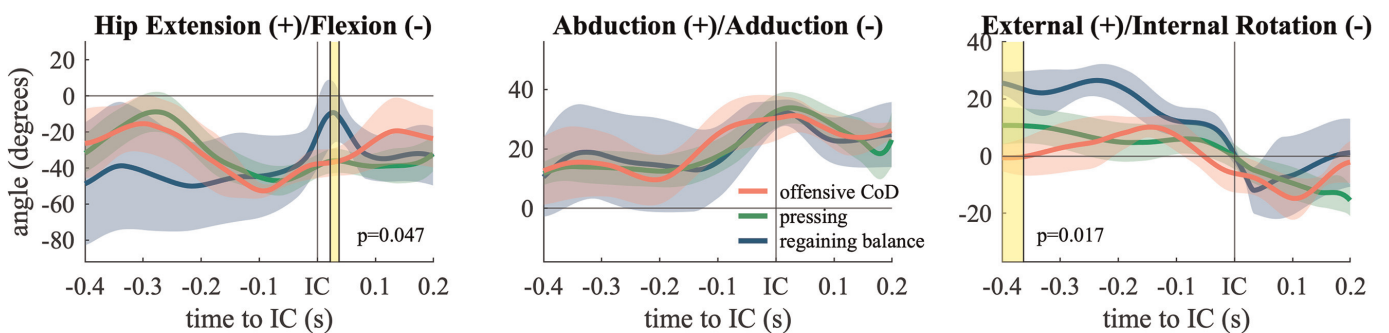


Figure 6. Hip joint kinematics (mean and SD) in the (left) sagittal, (center) frontal, and (right) transverse planes. Colors refer to separate situational patterns. Shaded bars indicate significant differences between patterns (1-dimensional analysis of variance). CoD, change of direction; IC, initial contact.

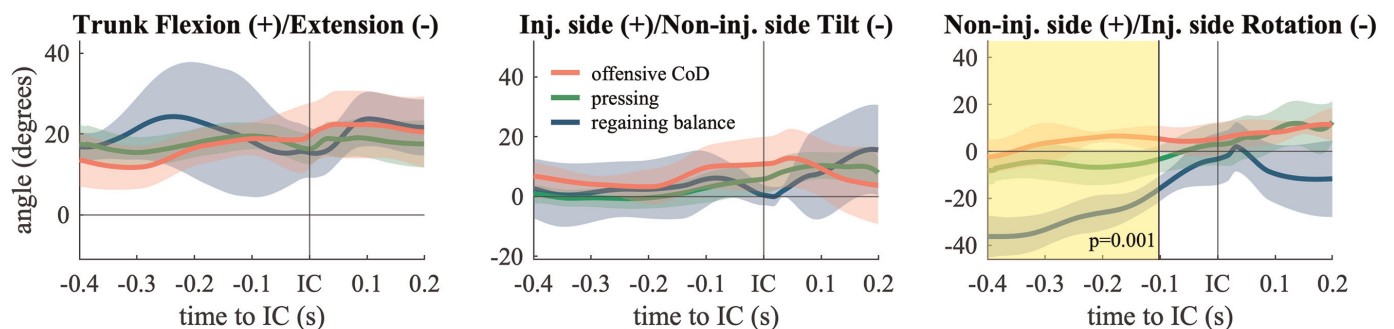


Figure 7. Trunk kinematics (mean and SD) in the (left) sagittal, (center) frontal, and (right) transverse planes. Colors refer to separate situational patterns. Shaded bar indicates a significant difference between patterns (1-dimensional analysis of variance). CoD, change of direction; IC, initial contact; Inj, injury.

(recovery balance) or adopting a slightly abducted posture (in the cases of pressings and offensive CoDs). At IC, the knee abduction (valgus) angle ranged from 1.1° to 3.6°.

In the transverse plane, all 3 patterns were displayed, with different ranges. There was a sudden external rotation (up to 5°), followed by a sudden internal rotation, which was largely completed by 100 ms from IC, when external (positive values) rotation spanned from -0.8° to 2.6°.

Hip Joint. In regaining balance injuries (Figure 6), the hip was less flexed 23 to 38 ms after IC (22.2° vs 37.7°-39.1°; $P = .047$).

In all 3 patterns, the hip was progressively abducted from about 200 ms before IC to a peak of 30° to 33° (SD, 8.1°).

In offensive CoDs, the hip was significantly less externally rotated (almost neutral) than in the other 2 patterns from 433 to 363 ms before IC ($P = .017$). The mean hip

rotation at IC ranged from -0.1° to 6.0° ; after IC, the hip remained externally rotated in all 3 patterns.

Trunk. Trunk flexion exhibited a high degree of variability (standard deviation range), particularly in regaining balance injuries. In the approach to and following IC, we observed 15° to 20° of forward trunk flexion for all 3 patterns (Figure 7).

Although the trunk was more inclined toward the injured side during offensive CoDs ($10.9^\circ \pm 8.9^\circ$ vs $5.8^\circ \pm 6.3^\circ$ for pressing injuries), this trend was not statistically significant.

In contrast, the trunk was significantly more rotated toward the noninjured side during recovery balance actions (ranging from -37° to -20°) and subtly rotated toward the injured side during offensive CoDs ($P = .001$) from 400 to 102 ms before IC. At IC, the trunk was rotated between -3.3° and 5.4° .

Noninjured Limb. Panels detailing the full 3D kinematics of the noninjured limb can be found in the Appendix Figure A4 (available online). In general, early differences (ie, preceding IC) between patterns were observed: at the hip level, being more abducted in recovery balance and internally rotated in pressing and offensive CoDs; and at the knee and ankle level, being more (plantar-)flexed in recovery balance patterns.

During and immediately after IC, the contralateral hip was more externally rotated in offensive CoDs, the contralateral knee was more internally rotated in recovery balance, and the ankle was more pronated in offensive CoDs.

Detailed representative total-body postures 300 ms before IC are available in the Appendix Figure 5A (available online).

DISCUSSION

This paper provides a detailed description of 3D joint kinematics preceding and during ACL injury events in male professional soccer players. The key advancements established are 2-fold: (1) reconstruction of joint angles offers a comprehensive and quantitative view of the kinematic conditions and body posture that led to injuries, partly confirming and significantly enriching the current knowledge on ACL injury biomechanics in soccer, and (2) ACL injury biomechanics in elite soccer changes according to the situational pattern.

Bidimensional video analyses have significantly augmented our awareness, representing to date the only practically viable ecological method to describe injury biomechanics. However, the MBIM technique has the potential to unveil subtle or time-dependent features that remain unclear or overlooked.^{18,19,21} To the best of our knowledge, only 3 papers have been published on MBIM and ACL injuries,¹⁸⁻²⁰ and just 1 case report has been published on MBIM in a professional soccer player,¹⁷ where the considered action cannot be considered representative of ACL injuries in soccer. The situational patterns analyzed in this current study included single-leg landings and unanticipated sidestepping tasks, which are most representative of noncontact ACL injury scenarios in soccer.^{8,12,37}

Knee Joint Kinematics

In all situational patterns, the knee was progressively extending in the phase preceding IF and then flexed afterward. A pronounced valgus trend (knee abduction) was observed, as expected, after IC. Flexing the knee during the loading response typically occurs in CoDs and landing tasks.^{1,14,41} This entails an eccentric (braking) action of the knee extensors, which are primarily responsible for reducing the body momentum, counteracting an external knee flexion moment.^{1,5,6} Although it is recognized that knee postures approaching full extension increase the ACL loading, assuming all other variables are unchanged,²⁶ we found that the knee was flexed to approximately 40° at IC, a higher value than previously reported. In 2020, Della Villa and colleagues,⁸ via 2-dimensional (2D) video analysis on a larger analogous cohort, found a similar knee flexion value at the suspected IF, while at IC they reported a knee more extended by approximately 20° , in line with the work by Koga et al¹⁹ on handball players (Appendix Figure A6, available online). This discrepancy can possibly be explained by the different nature of the surface (stiffer in the handball field), specific shoe-ground interaction, and different technical actions involved in ACL injuries in handball.

It is commonly accepted that the ACL rupture occurs between 40 and 80 ms after IC. In our results, the phase of knee abduction began slightly before IC and persisted for approximately 150 ms, up to 100 ms after IC. At the same time, the knee was rapidly externally and subsequently internally rotated.

We must consider that our joint angles represent the relative rotations of the distal segment with respect to the proximal one. As the injured limb is constrained to the ground, the sequence of external-internal knee joint rotations corresponds to a sudden internal-external rotation of the femur, the first (internal) rotation occurring during loading acceptance. We argue that this could be the critical situation that leads to the ACL injury. The subsequent external rotation of the femur, associated with knee abduction, could be interpreted as the response to the loss of structural integrity caused by the ligament failure, having a "rebound" in both the frontal and the transverse planes.

These findings complement the current knowledge on the role of the external valgus moment.^{13,31,33,38} Also, they corroborate the hypothesis of an externally applied internal rotation moment, which was supposed to be applied to the knee undergoing the ACL failure,¹ despite this historically being an inconsistent or controversial point. Notably, such internal tibial torque generated by an external reaction force likely produced the observed internal knee rotation, while the knee had previously been externally rotated (Figure 5, right panel).³³

Furthermore, we present evidence that a net valgus shift (likely produced by an external valgus moment, exceeding the internal balancing muscle stabilization) is applied throughout the entire duration from IC to IF, alongside an internal rotation moment (technically, an external moment produced by the ground-reaction forces

transmitted throughout the kinetic chain from the ankle to the knee). Just after IC, when the loading is still incomplete, knee stabilizers manage to externally rotate the knee. However, once the load increases (about 30 ms after IC), the external load is unmatched, and the knee rapidly collapses. We argue that the combination of a swift external-internal rotation, paired with a valgus angle, knee compression, and external flexion moment, ultimately leads to injury.

To our knowledge, this is the first time this abrupt knee external rotation has been documented. This observation gains clarity when considering the biomechanical context: during this phase, the foot is constrained to the ground; simultaneously, the knee shifts toward a valgus angle, while the hip undergoes adduction and internal rotation. Indeed, a quick change in hip rotation is observed, as expected, synchronizing with knee kinematics during the same time frame.

Whole-Body Kinematics

The orientation and stabilization of the ankle have a huge effect on how loads are transferred to proximal segments. In this study, we found the ankle to be predominantly externally rotated during recovery balance actions, in agreement with the traditional assumption that the ankle is externally rotated during ACL injuries. In contrast, we found that it was internally rotated during pressing and offensive CoDs, which were mostly sidestepping actions.

An extended hip during recovery balance can be attributed to the concurrent landing maneuver, often performed with a tendency toward a more extended limb compared with the other 2 patterns (see Figure 6). We confirmed a clear hip abduction (up to $\sim 30^\circ$ at IC), but we observed notable differences in hip rotation (almost neutral in offensive CoDs). During the ground contact phase (IC to IF and onward), the hip was internally rotated in all 3 patterns, an intersegmental relationship that exacerbated the knee valgus behavior. The trunk was flexed forward, tilted toward the injured side, and rotated in the same direction (except for offensive CoDs). Laboratory biomechanical studies^{6,34,37} have shown that this combination enhances the moment arm of the ground-reaction forces in the frontal plane, thereby increasing valgus knee loading.

The differences observed among situational patterns on the contralateral limb reinforce the idea that the causal pathway leading to injury is not unique.

Methodological Implications: An Ecologic Perspective

Overall, we found consistent knee mechanics across situational patterns. However, the intersegmental relationship at the surrounding joints, as well as the history of joint kinematics, was context dependent. More specifically, we found that environmental constraints and game-specific demands influenced the arrangement of body segments and, in turn, distinct motor programming and neuromuscular coordination (including the steps before the last one). These conditions resulted in separate motion pathways, all driving to excessive knee loading.

Furthermore, the rate of joint kinematic change is critical. We unveiled a complex sequence of events happening at the knee joint in <100 ms, that is, a sudden inversion in rotation direction from external to internal, accompanied by increased flexion and abduction. Mechanically, ligaments exhibit a viscoelastic behavior; thus, quick multiplanar inversion can increase the ligament stress and decrease the amount of energy that the tissue can absorb.²²

Traditional injury prevention programs have demonstrated their effectiveness in injury mitigation,³⁶ but at the same time they are challenged by increased exercise demands. Thus, we hereby propose a shift from general strengthening and stability control exercises toward a discipline-specific approach that gradually exposes players to both dynamic (and realistic) situational demands and sidestepping/landing at speed. The underlying principle is that education on a safe running/turning/sidestepping technique in a complex environment is akin to teaching and improving technical skills.^{3,7} As such, the closer the training is to the reality of the game, the more effective it becomes.²⁵

Limitations and Technical Considerations

To the best of our knowledge, this is the largest study on ACL injury mechanism ever conducted with the MBIM technique. Although it allows for a thorough reconstruction of the injurious actions and it is in principle more reliable than traditional 2D video analysis, this technique is not exempt from potential issues. A first source of uncertainty is that the precise time of the injury is not known. Even if, as described below, we made all the viable efforts to ensure our estimate was accurate, this time point could be shifted in reality by fractions of the sampling time.

Second, it is highly time-consuming. The camera calibration stage is critical; must be performed manually; and can be affected by image quality, occlusions, lens distortion, continuous focal length changes (ie, zooming) during the action, and the number of known references on the multiple views (especially on a closed-field view). To mitigate the effects of these potential confounders, we discussed the camera positioning and settings with professional Serie A camera managers, and the calibration was always performed by 2 operators working together. The same approach was applied to posture matching, which was conducted by 2 investigators and independently checked and adjusted by 2 additional investigators.

This redundant and meticulous approach to limiting the interoperator subjectivity in pose reconstruction could not be entirely eliminated, an objective technical difficulty in matching the model from multiple camera views. It is crucial to note that MBIM, while providing valuable insights, is not a measure but rather an estimate and involves inherent approximations. The measurement uncertainty was previously estimated in a study by Krosshaug and Bahr²¹: about 3° to 8° (sagittal plane), 1° to 7° (frontal plane), and 3° to 9° (transverse plane),¹⁶ substantially lower than in 2D video analysis. Last, inaccuracies from individual frames were unlikely to compound across multiple measurements, as each frame/case was treated

independently and the averaging of individual curves reduced the effect of the uncertainty on the final results.

Statistical power of comparisons might be affected by the uneven distribution of cases among the situational pattern classes, but this reflects the actual proportion of non-contact injuries in elite soccer.⁸

Unlike a previous case report,¹⁷ we set the skeletal model to block the translational degrees of freedom of all the joints, knee included, as we deemed it practically unfeasible to reproduce the small tibiofemoral displacements reliably and consistently in all 33 cases.

Finally, this analysis was intentionally restricted to ACL biomechanics. Contextual factors other than the game situation (eg, location on the pitch, score at the time of injury, game time, external perturbations, and workload) can dynamically alter an athlete's susceptibility to injury²⁹ and, consequently, one's behavior on the pitch. Further considerations of these factors are required to provide a global perspective on the injury action and are going to be addressed in future works.

CONCLUSION

In this study, we provided a detailed and nuanced description of multiplanar features (transverse and coronal plane rotations) on the injury kinematics preceding and during the injury action. We concluded that ACL injuries in male professional soccer players manifest via distinct biomechanical footprints that are related to the concurrent game situation—namely, offensive CoDs, pressing, and recovery balance actions.

ACKNOWLEDGMENT

The passion and commitment of the MSc degree students who have been working on this project over the years is gratefully acknowledged: Lorenzo Barbante, Laura Orione, and Alice Ranzini (biomedical engineers) and Eleonora Cacciatore, Martina Carcano, Alessandro Girelli, and Monica Nitri (sport scientists). The authors also thank Dr. Nicola Linguaglossa from NVP SpA for his availability and courtesy in explaining to them the structure of Serie A stadiums' camera plan.

ORCID iD

Matteo Zago  <https://orcid.org/0000-0002-0649-3665>

REFERENCES

1. Beaulieu ML, Ashton-Miller JA, Wojtyls EM. Loading mechanisms of the anterior cruciate ligament. *Sports Biomech.* 2023;22(1):1-29.
2. Bertozzi F, Fischer PD, Hutchison KA, Zago M, Sforza C, Monfort SM. Associations between cognitive function and ACL injury-related biomechanics: a systematic review. *Sports Health.* 2023;15(6):855-866.
3. Bittencourt NFN, Meeuwisse WH, Mendonça LD, Nettel-Aguirre A, Ocarino JM, Fonseca ST. Complex systems approach for sports injuries: moving from risk factor identification to injury pattern recognition—narrative review and new concept. *Br J Sports Med.* 2016;50(21):1309-1314.
4. Boden BP, Torg JS, Knowles SB, Hewett TE. Video analysis of anterior cruciate ligament injury. *Am J Sports Med.* 2009;37(2):252-259.
5. David S, Komnik I, Peters M, Funken J, Potthast W. Identification and risk estimation of movement strategies during cutting maneuvers. *J Sci Med Sport.* 2017;20(12):1075-1080.
6. David S, Mundt M, Komnik I, Potthast W. Understanding cutting maneuvers—the mechanical consequence of preparatory strategies and foot strike pattern. *Hum Mov Sci.* 2018;62:202-210.
7. Davids K. Principles of motor learning in ecological dynamics: a comment on functions of learning and the acquisition of motor skills (with reference to sport). *Open Sports Sci J.* 2012;5(1):113-117.
8. Della Villa F, Buckthorpe M, Grassi A, et al. Systematic video analysis of ACL injuries in professional male football (soccer): injury mechanisms, situational patterns and biomechanics study on 134 consecutive cases. *Br J Sports Med.* 2020;54:1423-1432.
9. Della Villa F, Esposito F, Busà M, Stillavato S, Zago M. The three-dimensional reconstruction of an Achilles tendon rupture in a professional football player reveals a multiplanar injury mechanism. *Knee Surg Sports Traumatol Arthrosc.* 2022;30(12):4198-4202.
10. Ekstrand J, Spreco A, Bengtsson H, Bahr R. Injury rates decreased in men's professional football: an 18-year prospective cohort study of almost 12 000 injuries sustained during 1.8 million hours of play. *Br J Sports Med.* 2021;55(19):1084-1092.
11. Gokeler A, Benjaminse A, Della Villa F, Tosarelli F, Verhagen E, Baumeister J. Anterior cruciate ligament injury mechanisms through a neurocognition lens: implications for injury screening. *BMJ Open Sport Exerc Med.* 2021;7(2):e001091.
12. Grassi A, Smiley SP, Roberti di, Sarsina T, et al. Mechanisms and situations of anterior cruciate ligament injuries in professional male soccer players: a YouTube-based video analysis. *Eur J Orthop Surg Traumatol.* 2017;27(7):967-981.
13. Hewett TE, Myer GD, Ford KR. Anterior cruciate ligament injuries in female athletes, part 1: mechanisms and risk factors. *Am J Sports Med.* 2006;34(2):299-311.
14. Hewett TE, Myer GD, Ford KR, Paterno MV, Quatman CE. Mechanisms, prediction, and prevention of ACL injuries: cut risk with three sharpened and validated tools. *J Orthop Res.* 2016;34(11):1843-1855.
15. Johnston JT, Mandelbaum BR, Schub D, et al. Video analysis of anterior cruciate ligament tears in professional American football athletes. *Am J Sports Med.* 2018;46(4):862-868.
16. Kingston B, Murray A, Norte GE, Glaviano NR. Validity and reliability of 2-dimensional trunk, hip, and knee frontal plane kinematics during single-leg squat, drop jump, and single-leg hop in females with patellofemoral pain. *Phys Ther Sport.* 2020;45:181-187.
17. Koga H, Bahr R, Myklebust G, Engebretsen L, Grund T, Krosshaug T. Estimating anterior tibial translation from model-based image-matching of a noncontact anterior cruciate ligament injury in professional football: a case report. *Clin J Sport Med.* 2011;21(3):271-274.
18. Koga H, Muneta T, Bahr R, Engebretsen L, Krosshaug T. Video analysis of ACL injury mechanisms using a model-based image-matching technique. In: Kanosue K, Ogawa T, Fukano M, Fukubayashi T, eds. *Sports Injuries and Prevention.* Springer Japan; 2015:109-120.
19. Koga H, Nakamae A, Shima Y, et al. Mechanisms for noncontact anterior cruciate ligament injuries. *Am J Sports Med.* 2010;38(11):2218-2225.
20. Koga H, Nakamae A, Shima Y, Bahr R, Krosshaug T. Hip and ankle kinematics in noncontact anterior cruciate ligament injury situations: video analysis using model-based image matching. *Am J Sports Med.* 2018;46(2):333-340.
21. Krosshaug T, Bahr R. A model-based image-matching technique for three-dimensional reconstruction of human motion from uncalibrated video sequences. *J Biomech.* 2005;38(4):919-929.
22. Kwan MK, Lin THC, Woo SLY. On the viscoelastic properties of the anteromedial bundle of the anterior cruciate ligament. *J Biomech.* 1993;26(4-5):447-452.
23. Lemme NJ, Li NY, Kleiner JE, Tan S, DeFroda SF, Owens BD. Epidemiology and video analysis of Achilles tendon ruptures in the National Basketball Association. *Am J Sports Med.* 2019;47(10):2360-2366.

24. Lucarno S, Zago M, Buckthorpe M, et al. Systematic video analysis of ACL injuries in professional women soccer players. *Am J Sports Med.* 2021;49(7):1794-1802.
25. Manolopoulos E, Papadopoulos C, Kellis E. Effects of combined strength and kick coordination training on soccer kick biomechanics in amateur players. *Scand J Med Sci Sports.* 2006;16(2):102-110.
26. Markolf KL, O'Neill G, Jackson SR, McAllister DR. Effects of applied quadriceps and hamstrings muscle loads on forces in the anterior and posterior cruciate ligaments. *Am J Sports Med.* 2004;32(5):1144-1149.
27. Montgomery C, Blackburn J, Withers D, Tierney G, Moran C, Simms C. Mechanisms of ACL injury in professional rugby union: a systematic video analysis of 36 cases. *Br J Sports Med.* 2018;52(15):994-1001.
28. Pataky TC, Robinson MA, Varenterghem J. Vector field statistical analysis of kinematic and force trajectories. *J Biomech.* 2013;46(14):2394-2401.
29. Pol R, Hristovski R, Medina D, Balague N. From microscopic to macroscopic sports injuries: applying the complex dynamic systems approach to sports medicine: a narrative review. *Br J Sports Med.* 2019;53(19):1214-1220.
30. Pulici L, Certa D, Zago M, Volpi P, Esposito F. Injury burden in professional European football (soccer): systematic review, meta-analysis, and economic considerations. *Clin J Sport Med.* 2023;33(4):450-457.
31. Quatman CE, Quatman-Yates CC, Hewett TE. A "plane" explanation of anterior cruciate ligament injury mechanisms: a systematic review. *Sports Med.* 2010;40:729-746.
32. Rafeeuddin R, Sharir R, Staes F, et al. Mapping current research trends on neuromuscular risk factors of non-contact ACL injury. *Phys Ther Sport.* 2016;22:101-113.
33. Santos CF, Bastos R, Andrade R, et al. Revisiting the role of knee external rotation in non-contact ACL mechanism of injury. *Applied Sci (Switzerland).* 2023;13(6):3802.
34. Song Y, Li L, Hughes G, Dai B. Trunk motion and anterior cruciate ligament injuries: a narrative review of injury videos and controlled jump-landing and cutting tasks. *Sports Biomech.* 2023;22(1):46-64.
35. Voskanian N. ACL injury prevention in female athletes: review of the literature and practical considerations in implementing an ACL prevention program. *Curr Rev Musculoskelet Med.* 2013;6(2):158-163.
36. Webster KE, Hewett TE. Meta-analysis of meta-analyses of anterior cruciate ligament injury reduction training programs. *J Orthop Res.* 2018;36(10):2696-2708.
37. Weir G. Anterior cruciate ligament injury prevention in sport: biomechanically informed approaches. *Sports Biomech.* Published online December 29, 2021. doi:10.1080/14763141.2021.2016925
38. Wojtys EM, Beaulieu ML, Ashton-Miller JA. New perspectives on ACL injury: on the role of repetitive sub-maximal knee loading in causing ACL fatigue failure. *J Orthop Res.* 2016;34(12):2059-2068.
39. Wu G, Cavanagh PR. ISB recommendations in the reporting for standardization of kinematic data. *J Biomech.* 1995;28(10):1257-1261.
40. Yona T, Kamel N, Cohen-Eick G, Ovadia I, Fischer A. One-dimension statistical parametric mapping in lower limb biomechanical analysis: a systematic scoping review. *Gait Posture.* 2024;109:133-146.
41. Zago M, David S, Bertozzi F, et al. Fatigue induced by repeated changes of direction in elite female football (soccer) players: impact on lower limb biomechanics and implications for ACL injury prevention. *Front Bioeng Biotechnol.* 2021;9:666841.